THE ASTROPHYSICAL JOURNAL, 396:711–716, 1992 September 10

SIMULTANEOUS VISIBLE AND NEAR-INFRARED SPECTROPHOTOMETRY OF COMET AUSTIN 1989c$_1$

STEPHEN C. TEGLER[1] AND HUMBERTO CAMPINS
Department of Astronomy, University of Florida, Gainesville, FL 32611
STEPHEN LARSON
Lunar and Planetary Laboratory, University of Arizona, Tucson, AZ 85721
MARVIN KLEINE
Department of Physics and Astronomy, Arizona State University, Tempe, AZ 85287
AND
DOUGLAS KELLY AND MARCIA RIEKE
Steward Observatory, University of Arizona, Tucson, AZ 85721
Received 1991 October 21; accepted 1992 March 10

ABSTRACT

Simultaneous visible and near-infrared spectra of comet Austin were obtained with the 1.5 m and 2.3 m telescopes of the University of Arizona Observatories on 1990 May 16. The visible spectrum obtained with the IHW spectrograph covers the 3126–9490 Å wavelength interval, while the near-infrared spectrum obtained with the germanium spectrometer covers the 9036–12794 Å wavelength interval. For the first time, we present simultaneous measurements of integrated band fluxes for the CN $B\ ^2\Sigma^+$–$X\ ^2\Sigma^+$ (violet) and $A\ ^2\Pi^+$–$X\ ^2\Sigma^+$ (red) systems. We also present a CN spectrum and CN band flux ratios calculated from a fluoresence equilibrium model. From a comparison between the observed and calculated CN spectra and band flux ratios, we find that red system oscillator strengths determined from recent ab initio calculations appropriately describe the radiative properties of CN molecules.

Subject headings: comets: individual (Austin 1989c$_1$) — molecular processes

1. INTRODUCTION

CN bands are observed in the spectra of comets to extend from the near-ultraviolet to the near-infrared. These bands involve transitions between the lowest three electronic states: $X\ ^2\Sigma^+$, $A\ ^2\Pi$, and $B\ ^2\Sigma^+$. Analysis of these bands results in a better understanding of comet formation. In particular, analysis of the $B\ ^2\Sigma^+$–$X\ ^2\Sigma^+$ (violet) system in high-resolution spectra of comets provides a measure of the $^{12}C/^{13}C$ abundance ratio in comets which provides a powerful discriminant between suspected condensation sites of comets (Wyckoff et al. 1989).

An accurate determination of the $^{12}C/^{13}C$ abundance ratio in comets from CN observations requires accurate values for the CN absorption oscillator strengths. The values for the oscillator strengths are determined from laboratory experiments or ab initio calculations. There is good agreement between experimental and theoretical determinations of the violet system oscillator strengths (Knowles et al. 1988; Cartwright & Hay 1982; Duric, Erman, & Larsson 1978; Danylewych & Nicholls 1978). However, values for the $A\ ^2\Pi$–$X\ ^2\Sigma^+$ (red) system oscillator strengths determined from laboratory experiments show large scatter. Specifically, laboratory experiments give values for the $X\ ^2\Sigma^+(v'' = 0) \rightarrow A\ ^2\Pi(v' = 0)$ oscillator strength that vary between 1.9×10^{-3} and 5.9×10^{-3} (Davis et al. 1986; Sneden & Lambert 1982; Duric et al. 1978; Treffers 1975; Arnold & Nicholls 1972; and Jeunehomme 1965). Recent ab initio calculations of values for the red system oscillator strengths are in very good agreement (Knowles et al. 1988; Bauschlicher, Langhoff, & Taylor 1988; and Lavendy, Gandara, & Robbe 1984).

Observations of CN bands in low-resolution spectra of comets provide an opportunity to determine whether or not values for oscillator strengths determined from ab initio calculations accurately describe the radiative properties of CN molecules. Consider the interaction of cometary CN molecules with solar photons, which excite the internal degrees of freedom (electronic, vibrational and rotational) of CN. The excited CN molecules subsequently reemit one or several photons producing emission lines. Since the CN molecules absorb and reemit many photons before being photodissociated by solar photons, the distribution of CN molecules over vibrational and rotational states in electronic states is time-independent. The vibrational and rotational populations may be predicted by solving a system of equations. An equation exists for each state requiring that the transition rate into a state is equal to the transition rate out of a state. The transition rates between states are calculated from the absorption oscillator strengths. A spectrum may be calculated from the population distribution and compared to an observed spectrum. A favorable comparison between observed and calculated spectra indicates the set of oscillator strengths accurately describes the radiative properties of CN molecules.

Danks & Arpigny (1973), Schleicher (1983), and Zucconi & Festou (1985) calculated spectra for CN molecules in the comae of comets. These investigators were unable to rigorously constrain values for the red system oscillator strengths because of the lack of an observed comet spectrum containing both the violet and red systems. The brightest bands of the violet and red systems occur at 3883 Å and 10930 Å, respectively. To obtain such a spectrum requires that two spectrom-

[1] Current postal address: Department of Physics, University of Notre Dame, Notre Dame, IN 46556.

eters be used since no one detector is sensitive over such a wide wavelength interval. In addition, the two spectrometers need to be used simultaneously since the integrated band fluxes from comets have been observed to vary by more than a factor of 2 during a 24 hr period (e.g., Tegler & O'Dell 1987).

We present simultaneous visible and near-infrared spectrophotometric observations of a comet for the first time. We compare these observations with a fluorescence equilibrium model and show that values for the violet and red system oscillator strengths determined from recent ab initio calculations closely describe the radiative properties of CN molecules.

2. OBSERVATIONS

2.1. *Visible*

We obtained simultaneous visible and near-infrared spectra of comet Austin with the 1.5 m and 2.3 m telescopes of the University of Arizona Observatories on 1990 May 16 UT during photometric conditions. At the time of our observations the heliocentric and geocentric distances of comet Austin were 0.979 and 0.304 AU, respectively. Also, comet Austin showed little day-to-day variability at the time of our observations.

We used the 1.5 m telescope at the Catalina Observatory near Mount Bigelow to obtain 3216–9490 Å long-slit spectra with the IHW CCD camera/spectrograph and a 158 line mm^{-1} grating blazed at 3500 Å that produced a dispersion of about 12 Å per pixel. The slit dimensions were 2.″5 by 200″ on the sky. The slit width and optical aberrations produced an effective mean resolution (FWHM) of about 45 Å. The spatial scale along the slit was 0.″7 $pixel^{-1}$.

The photocenter of comet Austin was placed at the center of the slit whose long axis was oriented along the projected solar radius vector. The solar analog star SAO 107706 was observed at nearly the same air mass as the comet (<0.03 difference). The SAO 107706 spectrum indicated a seeing point spread function of about 1.″5 (FWHM). The spectra of SAO 107706 were immediately followed by slitless spectra from which we estimated that 75% of the total flux of a point source entered the slit.

The comet Austin CCD spectrum was bias-subtracted, divided by a dome flat field, wavelength-calibrated, and spatially rectified using IRAF. Seven columns (5″) centered on the peak brightness of the comet were extracted from the CCD spectrum and summed. The extracted spectrum was sky-subtracted. The sky spectrum was obtained earlier in the night as part of a 30 minute exposure of 1990 HA and hence the sky spectrum contains no contamination from comet emissions. The sky-subtracted spectrum of comet Austin was corrected for telluric absorption (SAO 107706) and flux-calibrated (SAO 107706). The dust continuum was subtracted from the comet Austin spectrum by subtracting a scaled Brault solar spectrum such that the comet continuum bandpasses came as close to zero as possible without going negative. The continuum band pass at 9000 Å went to zero and the continuum band passes at 3600 and 4400 Å were very close to zero, but not exactly. The reddening of the continuum was very small.

In Figure 1 we show the processed visible spectrum of comet Austin (*solid line*). We see in Figure 1 the violet system $\Delta v = 0$ and $\Delta v = -1$ band sequences at 3883 and 4216 Å, respectively, as well as the red (2–0), (3–1), and (1–0) bands at 7873, 8067, and 9141 Å, respectively.

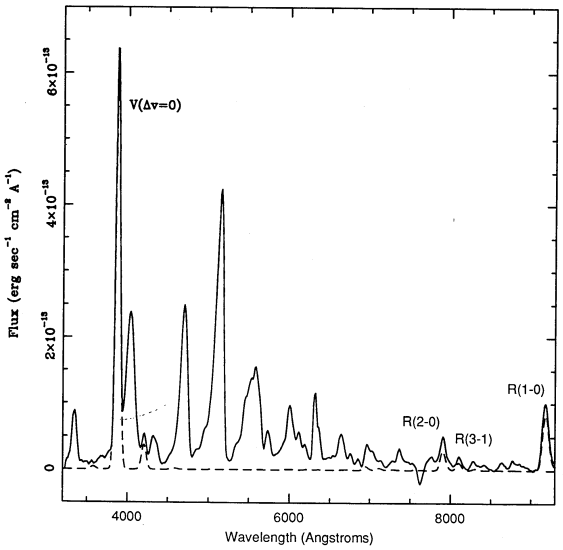

FIG. 1.—Visible spectrum of comet Austin obtained with the IHW spectrograph on the University of Arizona Observatories 1.5 m telescope (*solid line*). The spectrograph slit was oriented along the extended solar radius vector. The aperture extraction from the long-slit CCD spectrum was 1.″5 × 5.″0 projected on the plane of the sky and centered on the peak brightness of the comet. Both the sky brightness and the dust continuum have been subtracted from the spectrum. CN bands and band sequences are labeled. Calculated CN spectrum (*dashed line*).

2.2. *Near-Infrared*

We obtained 9036–12794 Å spectra with the germanium spectrometer on the 2.3 m telescope on Kitt Peak. GeSpec is a classical grating spectrometer with two germanium arrays in the plane of two spectra formed from double entrance apertures. The entrance apertures were 5″ holes with center separation of 1′. A 150 line mm^{-1} grating was used giving a resolution (FWHM) of 60 Å.

Comet Austin's photocenter was centered first in the left aperture, then the right aperture in sequence. SAO 107706 was also observed at near-infrared wavelengths and at an air mass very similar to the comet Austin air mass (~0.05 difference). In Table 1 we present the integration time per spectrum, number

TABLE 1

OBSERVATIONAL PARAMETERS

Object	Wavelength Interval (Å)	Integration Time Per Spectrum (s)	Number of Spectra
Comet Austin	3216–9490	600	1
	9036–9995	30	13
	9837–10795	30	13
	10636–11594	30	15
	11437–12395	30	15
	11837–12794	30	68
SAO 107706	3216–9490	10	1
	9036–9995	2	11
	9837–10795	2	13
	10636–11594	3	21
	11437–12395	3	9
	11837–12794	3	26

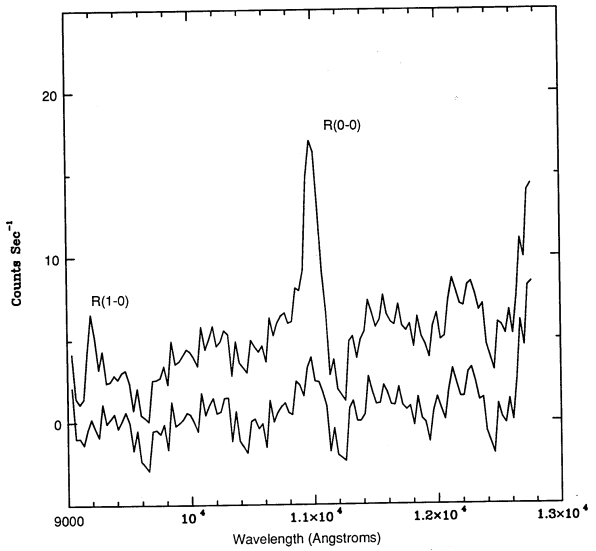

FIG. 2.—Near-infrared spectrum of comet Austin (*above*) and the sky (*below*) obtained with the dual-aperture germanium spectrometer on the University of Arizona Observatories 2.3 m telescope. These spectra include atmospheric absorptions and telescope and instrument responses. The comet Austin spectrum was obtained by placing the peak brightness of the comet at the center of a 5″ circular aperture. The sky spectrum was obtained 1′ offset from the peak brightness of the comet.

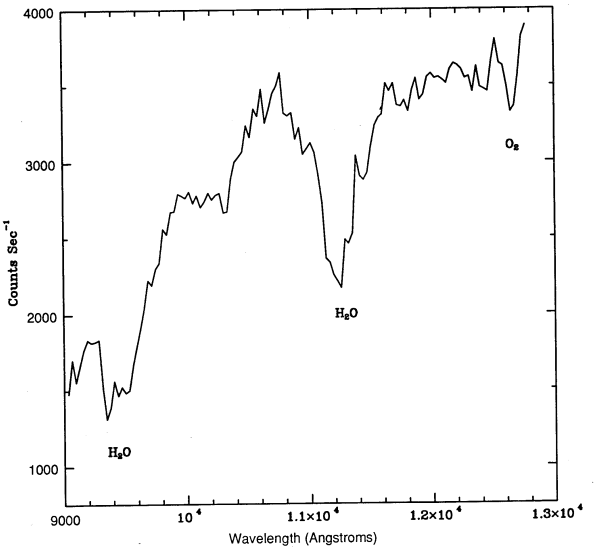

FIG. 3.—Near-infrared spectrum of SAO 107706 taken at air masses closely matching the comet Austin observations. The spectrum includes atmospheric absorptions and telescope and instrument responses.

of spectra, and the wavelength interval for the visible and near-infrared observations of comet Austin and SAO 107706.

The near-infrared observations were processed in the following manner. The infrared comet spectrum was first sky-subtracted. To minimize the temporal and spatial variability of the sky brightness at near-infrared wavelengths our sky spectrum was obtained 1′ from the peak brightness of the comet, i.e., we used the sky spectrum that resulted from beam switching. In Figure 2 we present spectra of comet Austin and the sky prior to data processing. From Figure 2 we see that at the R(0–0) band peak, the count rate in the sky spectrum is $\sim$20% of the count rate in the comet Austin spectrum. Since the sky spectrum has contributions from the sky brightness and the coma, the CN emission in the sky spectrum is less than 20% of the CN emission in the comet Austin spectrum. In Figure 3 we present a spectrum of SAO 107706 prior to data processing. The SAO 107706 spectrum in Figure 3 was sky-subtracted and normalized to count rates near unity. We flat-fielded and removed telluric absorption from the comet Austin spectrum by dividing the comet spectrum by the normalized SAO 107706 spectrum. We then multiplied the comet Austin spectrum by the instrumental sensitivity function to obtain a flux-calibrated comet Austin spectrum in units of ergs s^{-1} cm^{-2} Å^{-1}. The sensitivity function was obtained by dividing the spectral energy distribution of SAO 107706 at the top of the Earth's atmosphere in units of ergs s^{-1} cm^{-2} Å^{-1} by the spectrum of SAO 107706 (sky-subtracted, flat-fielded, and corrected for telluric absorption). The spectral energy distribution of SAO 107706 was calculated from a V magnitude of 6.18, a $V-J$ color of 1.03, and a blackbody function with $T = 5900$ K. The spectral type and V magnitude for SAO 107706 were taken from the Smithsonian Astrophysical Observatory Star Catalog. In Figure 4 we present the flux-calibrated comet Austin spectrum. Since Fraunhofer lines in the near-infrared spectrum of the Sun are negligible, we subtracted the continuum emission from the comet Austin spectrum by subtracting a polynomial such that the continuum bandpasses of the comet spectrum went to zero.

In Figure 5 we show the continuum-subtracted spectrum of comet Austin (*solid line*). We see in Figure 5 the CN red (1–0), (2–1), and (0–0) bands at 9141, 9381, and 10930 Å, respectively. In addition, we see in Figure 5 the C_2 $A\ ^1\Pi_u$–$X\ ^1\Sigma_g^+$ (Phillips)

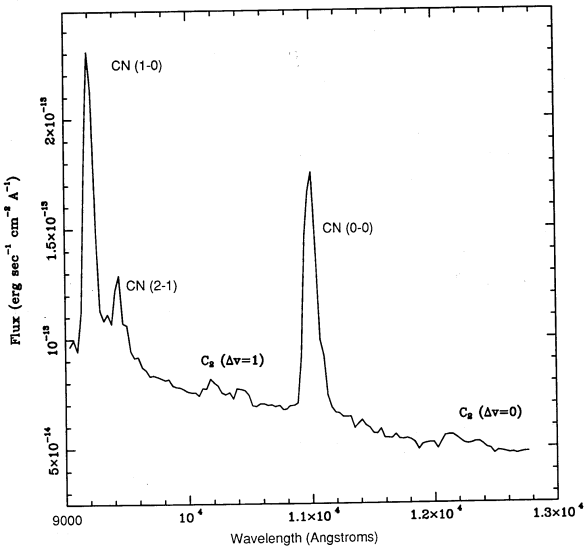

FIG. 4.—Flux-calibrated near-infrared spectrum of comet Austin. Atmospheric absorptions and telescope and instrument responses have been removed. CN bands and C_2 band sequences are labeled. The dust continuum has not been subtracted.

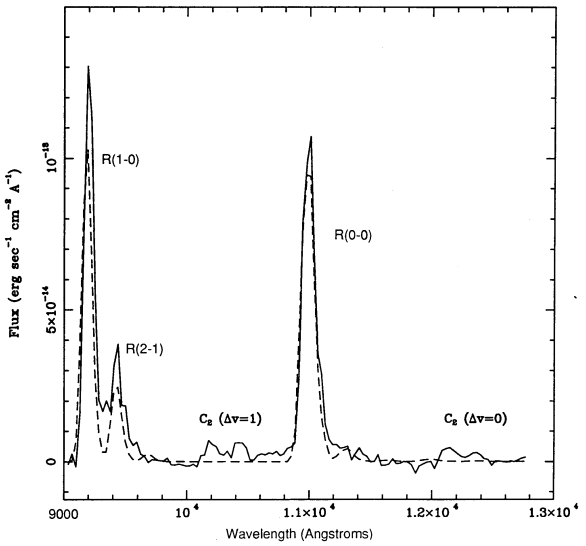

FIG. 5.—Flux-calibrated near-infrared spectrum of comet Austin (*solid line*). The dust continuum has been subtracted. Calculated CN spectrum (*dashed line*).

$\Delta v = 1$ band sequence at 10100 Å, reported here for the first time in a comet. The C_2 Phillips $\Delta v = 0$ band sequence at 12100 Å is also present and has been observed once previously in a comet (Johnson, Fink, & Larson 1983).

2.3. *Band Fluxes*

The visible and near-infrared spectra were processed independently. The measured $R(1–0)$ integrated band flux in the visible and near-infrared spectra were found to differ by 15%. We measured $R(1–0)$ band fluxes of 1.0×10^{-11} and 1.27×10^{-11} ergs s^{-1} cm^{-2} from the visible and near-infrared spectra, respectively. Since we were interested in the relative difference between the red and violet system bands and the $R(1–0)$ band flux should be identical in both spectra, we multiplied the band fluxes in the near-infrared spectrum by the ratio of the visible to near-infrared $R(1–0)$ band flux. The integrated CN band fluxes are presented in Table 2.

At the resolution of our observations, the observed violet and red bands are blended with other molecular bands. In particular, the $V(\Delta v = 0)$ band is blended with the C_3 band at 4040 Å and the $V(\Delta v = -1)$ band is blended with the CH (0–0) band at 4315 Å. The $R(2–0)$ and $R(3–1)$ bands are blended with the C_2 Phillips ($\Delta v = 3$) band sequence and the $R(1–0)$ and $R(2–1)$ bands are blended with the C_2 Phillips ($\Delta v = 2$) band sequence. Uncertainties in our band flux measurements are primarily due to blending and are given in Table 2.

In Table 3 we present measured CN band flux ratios for comet Austin (col. [2]). The $V(\Delta v = 0)/R(0–0)$, $R(2–0)/R(0–0)$, and $R(3–1)/R(0–0)$ band flux ratios have not been measured previously. The $R(1–0)/R(0–0)$ and $R(2–1)/R(0–0)$ have been measured previously and show considerable scatter. Johnson et al. (1983) and Maillard et al. (1987) have measured the $R(1–0)/R(0–0)$ band flux ratio and obtained 0.45 and 1.70. Johnson et al. (1983), Johnson et al. (1984), and Maillard et al. (1987) have measured the $R(2–1)/R(0–0)$ band flux ratio and obtained 0.33, 0.26, 0.58, and 0.25. For investigators interested in the C_2 molecule, we present C_2 band sequence fluxes in Table 4 and C_2 band sequence flux ratios in Table 5.

TABLE 2

CN INTEGRATED BAND FLUXES

Band	Wavelength (Å)	Band Flux (ergs s^{-1} cm^{-2})
$V(\Delta v = 0)$	3883	$(4.4 \pm 0.4) \times 10^{-11}$
$V(0–1)$	4216	$(3.0 \pm 0.5) \times 10^{-12}$
$R(2–0)$	7873	$(3.3 \pm 0.5) \times 10^{-12}$
$R(3–1)$	8067	$(1.1 \pm 0.2) \times 10^{-12}$
$R(1–0)$	9141	$(1.0 \pm 0.05) \times 10^{-11}$
$R(2–1)$	9381	$(3.5 \pm 0.7) \times 10^{-12}$
$R(0–0)$	10930	$(1.1 \pm 0.06) \times 10^{-11}$

TABLE 3

RATIO OF CN BAND FLUXES

Band Flux Ratio (1)	Observed (2)	Calculated (3)
$\frac{V(\Delta v = 0)}{R(0–0)}$	3.8 ± 0.6	3.88
$\frac{R(2–0)}{R(0–0)}$	0.28 ± 0.05	0.23
$\frac{R(3–1)}{R(0–0)}$	0.10 ± 0.02	0.09
$\frac{R(1–0)}{R(0–0)}$	0.86 ± 0.10	0.79
$\frac{R(2–1)}{R(0–0)}$	0.30 ± 0.10	0.20

TABLE 4

C_2 INTEGRATED BAND SEQUENCE FLUXES

Band Sequence	Wavelength (Å)	Band Flux (ergs s^{-1} cm^{-2})
Swan ($\Delta v = +1$)	4737	$(3.0 \pm 0.3) \times 10^{-11}$
Swan ($\Delta v = 0$)	5165	$(6.0 \pm 0.6) \times 10^{-11}$
Swan ($\Delta v = -1$)	5636	$(3.5 \pm 0.4) \times 10^{-11}$
Phillips ($\Delta v = +1$)	10100	$(1.7 \pm 0.3) \times 10^{-12}$
Phillips ($\Delta v = 0$)	12100	$(8.4 \pm 1.6) \times 10^{-13}$

TABLE 5

RATIO OF C_2 BAND SEQUENCE FLUXES

Band Sequence Flux Ratio	Observed
$\frac{\text{Swan } (\Delta v = +1)}{\text{Swan } (\Delta v = 0)}$	0.51 ± 0.07
$\frac{\text{Swan } (\Delta v = -1)}{\text{Swan } (\Delta v = 0)}$	0.59 ± 0.08
$\frac{\text{Phillips } (\Delta v = +1)}{\text{Swan } (\Delta v = 0)}$	0.029 ± 0.007
$\frac{\text{Phillips } (\Delta v = 0)}{\text{Swan } (\Delta v = 0)}$	0.014 ± 0.003

3. THEORY

In this section, we describe the fluorescence equilibrium model used to predict CN band luminosities and the CN spectrum for comet Austin on 1990 May 16. The model predicts band luminosities and a spectrum by determining the distribution of CN molecules over vibrational and rotational states in the three lowest electronic states. The luminosity per molecule, L_{ij}, resulting from spontaneous transitions between states i and j is determined from

$$L_{ij} = A_{ij} N_i \frac{hc}{\lambda_{ij}}, \quad (1)$$

where A_{ij} is the Einstein coefficient for spontaneous emission, h is Planck's constant, c is the speed of light, λ_{ij} is the wavelength corresponding to the transition, and N_i is the normalized equilibrium population of state i. The equilibrium populations of the states are determined by solving a system of n linear equations where n is the total number of energy states. In equilibrium the number of transitions into a state is equal to the number of transitions out of a state

$$\sum_{i=j+1}^{n} (A_{ij} N_i - B_{ji} \rho_{ij} N_j) - \sum_{i=1}^{j-1} (A_{ji} N_j - B_{ij} \rho_{ij} N_i) = 0, \quad (2)$$

where ρ_{ij} is the solar radiation density and B is the Einstein coefficient for absorption. The Einstein A and B coefficients are related to the oscillator strengths, f_{ij}, by

$$A_{ij} = \frac{8\pi^2 e^2}{mc} \nu_{ij}^2 \frac{(2 - \delta_{0,\Lambda''})}{(2 - \delta_{0,\Lambda'})} f_{ij} \quad (3)$$

and

$$B_{ij} = \frac{\pi^2 e^2}{h m_e c} \frac{1}{\nu_{ij}} f_{ij}, \quad (4)$$

where ν_{ij} is the wavenumber corresponding to the $i \rightarrow j$ transition.

We have used the fluorescence equilibrium model developed by Kleine (1991), absorption oscillator strengths calculated by Knowles et al. (1988), and the solar flux atlas of Kurucz et al. (1984) to calculate CN band luminosities and a CN spectrum for comet Austin. In our calculation each electronic state ($X\ ^2\Sigma^+$, $A\ ^2\Pi$, and $B\ ^2\Sigma^+$) is modeled as a set of six vibrational levels containing 22 rotational levels each. The spin multiplicity of the CN radical splits each level further. In addition, each energy level in the $A\ ^2\Pi$ electronic state is split due to Λ-type doubling. A total of 1020 energy levels are included in our calculation. All allowed rotational-vibrational transitions between electronic states are included. Transition rates between electronic states are of the order 10^6–10^9 s^{-1}. Transition rates for pure rotational and vibrational transitions within these electronic states are negligible in comparison. Therefore, pure rotational and vibrational transitions are only included in the ground electronic state.

Besides the values for absorption oscillator strengths and the solar spectrum, the heliocentric radial velocity of the comet, $\dot{R}$, is an input parameter in the fluorescence model. Specifically, the solar spectrum has Fraunhofer lines and because of the Doppler effect the solar flux available to excite CN molecules in the ground electronic state depends on $\dot{R}$. Swings (1941) showed that the observed structure of the $V(\Delta v = 0)$ band is sensitive to $\dot{R}$. Violet system bands are more sensitive to $\dot{R}$ than red system bands because the near-infrared solar spectrum does not have strong Fraunhofer lines. In our calculation we have used the heliocentric radial velocity of comet Austin on 1990 May 16, 34.14 km s^{-1}.

We have calculated a CN spectrum that spans the 3216–12794 Å wavelength interval. In all, approximately 17,000 individual line intensities were computed. The calculated line intensities have been convolved with the instrumental response of the appropriate spectrometer. We have obtained the instrumental response of the spectrometers by measuring arc line profiles. To compare the calculated and observed CN bands we have normalized the calculated spectrum to the observed spectrum. In particular, we multiplied the calculated spectrum by the ratio of the observed to calculated $V(\Delta v = 0)$ fluxes. We show in Figures 1 and 5 the calculated CN spectrum for comet Austin (*dashed line*). The calculated band flux ratios are listed in Table 3.

4. DISCUSSION

In this section we compare the observed and calculated CN spectra and band flux ratios. We infer from the comparison how well the red system oscillator strengths calculated by Knowles et al. (1988) describe the radiative properties of CN molecules. We see in Figures 1 and 5 that the calculated CN spectrum (*dashed line*) compares very well with the observed CN spectrum (*solid line*). The bandpasses used in the observed spectrum to determine band fluxes were also used in the calculated spectrum to determine band fluxes. In Table 3 we see that the observed (col. [2]) and calculated (col. [3]) band flux ratios differ by only ~10%–20%. The difference between the observed and calculated band flux ratios is likely due to uncertainties in the measured CN band fluxes; the uncertainties in the measured band flux ratios overlap the calculated band flux ratios. Because the measurement uncertainty results mainly from blending of C_2 and C_3 bands with the CN bands, we are unable to refine the calculated values for the red system oscillator strengths; higher resolution observations may allow such a refinement.

From the good agreement between the observed and calculated spectra we conclude that red system oscillator strengths calculated by Knowles et al. (1988) closely describe the radiative properties of the CN red system. In Table 6 we compare CN oscillator strengths calculated by Knowles et al. (1988) with CN oscillator strengths calculated by other investigators for the CN bands in our spectra of comet Austin. From Table 6 we see that the oscillator strengths calculated by Bauschlicher et al. (1988) and Lavendy et al. (1984) are in very close agreement with the values calculated by Knowles et al. and hence also closely describe the radiative properties of the CN red

TABLE 6

OSCILLATOR STRENGTHS[a]

Band	f[b]	f[c]	f[d]
V(0–0)	34.5	...	29.0
V(0–1)	2.67	...	2.39
R(2–0).....	0.90	0.91	0.93
R(3–1).....	1.34	1.35	1.37
R(1–0).....	1.90	1.91	1.91
R(2–1).....	1.36	...	1.37
R(0–0).....	2.37	2.36	2.32

[a] Multiply values in table by 10^{-3}.
[b] Knowles et al. 1988.
[c] Bauschlicher, Langhoff, & Taylor 1988.
[d] Lavendy, Gandara, & Robbe 1984.

system. We suggest that these oscillator strengths be used in the analysis of CN bands observed in the spectra of astrophysical objects.

We thank John Black and an anonymous referee for useful comments on the manuscript. This research is supported by the University of Florida Division of Sponsored Research.

REFERENCES

Arnold, J. O., & Nicholls, R. W. 1972, J. Quant. Spectros. Rad. Transf., 12, 1435
Arpigny, C. 1964, Ann. d'Astrophys., 27, 393
Bauschlicher, C. W., Jr., Langhoff, S. R., & Taylor, P. R. 1988, ApJ, 332, 531
Cartwright, D. C., & Hay, P. J. 1982, ApJ, 257, 383
Danks, T., & Arpigny, C. 1973, A&A, 29, 347
Danylewych, L. L., & Nicholls, R. W. 1978, Proc. R. Soc. Lond., A, 360, 557
Davis, S. P., Shortenhaus, D., Stark, G., Engelman, R., Jr., Phillips, J. G., & Hubbard, R. P. 1986, ApJ, 303, 892
Duric, D. L., Erman, R., & Larsson, M. 1978, Phys. Scripta, 18, 39
Jeunehomme, M. 1965, J. Chem. Phys., 42, 4086
Johnson, J. R., Fink, U., & Larson, H. P. 1983, ApJ, 276, 769
———. 1984, Icarus, 60, 351
Kleine, M. 1991, in preparation
Knowles, P. J., Werner, H. J., Hay, P. J., & Cartwright, D. C. 1988, J. Chem. Phys., 89, 7334
Larsson, M., Siegbahn, P. E. M., & Agren, H. 1983, ApJ, 272, 369
Lavendy, H., Gandara, G., & Robbe, J. M. 1984, J. Molec. Spectrosc., 106, 395
Maillard, J. P., Crovisier, J., Encrenaz, T., & Combes, M. 1987, A&A, 187, 398
Schleicher, D. 1983, Ph.D. dissertation, University of Maryland
Sneden, C., & Lambert, D. L. 1982, ApJ, 259, 381
Swings, P. 1941, Lick Obs. Bull., 19, 131
Taherian, M. R., & Slanger, T. G. 1984, J. Chem. Phys., 81, 3814
Tegler, S. C., & O'Dell, C. R. 1987, ApJ, 317, 987
Treffers, R. 1975, ApJ, 196, 883
Wyckoff, S., et al. 1989, ApJ, 339, 488
Zucconi, J. M., & Festou, M. C. 1985, A&A, 150, 180